ELSEVIER

Journal of Nuclear Materials 253 (1998) 196–202

journal of nuclear materials

Section 5. Fabrication and properties of ceramic breeder materials

Fabrication development of Li_2O pebbles by wet process

Kunihiko Tsuchiya [a,*], Katsuhiro Fuchinoue [b], Shigeru Saito [a], Kazutoshi Watarumi [b], Takemi Furuya [b], Hiroshi Kawamura [a]

[a] *Oarai Research Establishment, JAERI, Oarai-machi, Higashi-ibaraki-gun, Ibaraki 311-13, Japan*
[b] *Nuclear Fuel Industries Ltd., Tokai-mura, Naka-gun, Ibaraki 319-11, Japan*

Abstract

Lithium oxide (Li_2O) is one of the best tritium breeding materials. A small sphere of Li_2O is proposed in some designs of fusion blankets. Recently, reprocessing technology on irradiated ceramic tritium breeders was developed from the viewpoint of effective use of resources and reduction of radioactive wastes. The wet process is advantageous for fabricating small Li_2O pebbles from the reprocessed lithium-bearing solutions. Preliminary fabrication tests of Li_2O pebbles by the wet process were carried out. However, the density of the pebbles obtained was only 55%. Therefore, process improvement tests were performed in order to increase the density of Li_2O pebbles fabricated by this method. The improved process yielded Li_2O pebbles in the target range of 80–85% T.D. © 1998 Elsevier Science B.V.

1. Introduction

Investigations of fusion reactors have focused on the tritium breeding materials contained in the blanket because those characteristics will have a large effect on the reactor design. Ceramic tritium breeders such as Li_2O, $LiAlO_2$, Li_2ZrO_3, Li_2TiO_3 and Li_4SiO_4 have been considered as candidates for tritium breeding materials for fusion reactors [1,2]. Particularly, lithium oxide (Li_2O) is one of the best tritium breeders considering its high lithium density and high thermal conductivity [3,4]. A small pebble is the proposed form of Li_2O in the Japanese design of a fusion blanket in order to reduce thermal stress [5–8]. Recently, reprocessing technology on irradiated ceramic tritium breeders has been developed from the viewpoint of effective use of resources and the reduction of radioactive wastes [9]. A sol–gel or wet process method [10–12] is most advantageous for fabricating small Li_2O pebbles from the reprocessed lithium-bearing solution.

A preliminary fabrication test of Li_2O pebbles by a wet process was previously carried out. However, the maximum density of Li_2O pebbles was 55% T.D. in that test [13]. Therefore, tests were conducted in this study to adjust modifications of the aging condition, calcination condition, thermal decomposition condition, etc. in order to increase Li_2O pebble density.

2. Experimental

2.1. Materials

Li_2CO_3 powder feed stocks were obtained with a purity of 99.9%. from Cerac. Polyvinylalcohol (PVA) was used as the binder for the Li_2CO_3 powder.

2.2. Fabrication process

An important feature of the wet process was the use of Li_2CO_3 powder and PVA as starting materials to produce Li_2O pebbles. The process steps are shown as follows.

(1) Fabrication of gel-spheres: The liquid mixture of Li_2CO_3 and PVA was dropped in cooled acetone through a nozzle in order to form spheres.

(2) Calcination of gel-spheres: PVA in the gel-spheres was removed leaving Li_2CO_3 spheres.

(3) Thermal decomposition and sintering: The Li_2CO_3 spheres were heated in vacuum to form Li_2O and then sintered.

* Corresponding author. Tel.: +81-29 264 8369; fax: +81-29 264 8480; e-mail: tsuchiya@jmtr.oarai.jaeri.go.jp.

PII S0022-3115(97)00312-7

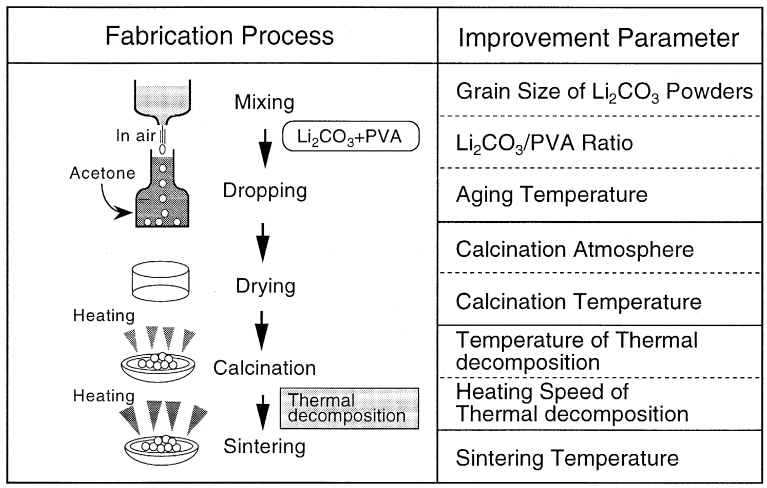

Fig. 1. A flow chart of the fabrication process of Li_2O pebbles and process improvement parameters.

A flow chart of the fabrication process of Li_2O pebbles and improvement parameters is shown in Fig. 1.

The developmental tests conducted were as follows:

In the first experiment, Li_2CO_3 powder was pulverized in order to reduce the grain size from 40 to 1.0 μm. In the process for fabrication of gel-spheres, the drop tests were carried out to decide the mixing ratio between Li_2CO_3 powder and PVA. In the second experiment, the effect of aging temperature in acetone on the density of Li_2CO_3 in the gel-spheres was evaluated. In the third experiment, heating tests were examined in order to remove PVA with the optimized gel-spheres and heating temperatures and atmospheres were decided. After the heating test, weight loss and growth of the grain size of the gel-spheres were measured and the crystal structure of the gel-spheres was analyzed by X-ray diffractometry (XRD). In the fourth and fifth experiments, thermal decomposition and sintering tests were carried out and the optimum condition for all parameters (heating temperature, heating rate, pressure, etc.) was demonstrated.

2.3. Characterization method of Li_2O pebbles

The characterization of Li_2O pebbles was performed by the methods described below. The density was measured by mercury porosimetry. The microstructure and crystalline form were determined by scanning electron microscopy (SEM) and XRD, respectively. The compressive failure load was measured using an unconfined compression tester with SiC compression indenter. The impurities in Li_2O pebbles were measured by atomic emission spectrometry with inductively coupled plasma (ICP-AES) and atomic absorption photometry and carbon content in Li_2O pebbles was measured by an infrared absorptiometric method.

Table 1
Summary of fabrication tests of Li_2O pebbles

Items	Process					
	size of Li_2CO_3 powders (μm)	aging temperature (°C)	calcination temperature (°C)	heating rate of thermal decomposition	sintering temperature (°C)	density (% T.D.)
Preliminary fabrication test	**40**	20	600	R.T. → 700°C, 1.7°C/min	1200	55
1st experiment	**1.0**	**20**	600	R.T. → 700°C, 3.3°C/min	1100	57
2nd experiment	1.0	**−20**	**600**	R.T. → 700°C, 3.3°C/min	1100	65
3rd experiment	1.0	−20	**400**	**R.T. → 700°C, 3.3°C/min**	1100	71
4th experiment	1.0	−70	400	**R.T. → 600°C, 3.3°C/min, 600°C → 700°C, 0.2°C/min**	**1100**	80
5th experiment	1.0	−70	400	R.T. → 600°C, 3.3°C/min, 600°C → 700°C, 0.2°C/min	**1150**	86

Bold type: Improvement parameters.

3. Results and discussions

3.1. Fabrication of Li_2O pebbles

A summary of fabrication tests of Li_2O pebbles is shown in Table 1. The results of each experiment in this process are described in Sections 3.1.1, 3.1.2 and 3.1.3.

3.1.1. Fabrication of gel-spheres

Li_2CO_3 powder was pulverized and the size of the Li_2CO_3 powder changed from 40 to 1.0 μm. The fabrication tests of gel-spheres were performed under various conditions involving the mixing ratio between the Li_2CO_3 powder and PVA, aging temperature and aging time in acetone. In these tests, Li_2CO_3 to PVA ratios of 26 and 5 wt% were chosen as the test parameters. The sphericity of gel-spheres fabricated with the pulverized Li_2CO_3 powder was better than that of gel-spheres fabricated with the Li_2CO_3 powder (40 μm). The grain size of gel-spheres was small. In the 2nd experiment, the aging temperature was evaluated. The aging temperature dependence on the density of Li_2CO_3 in gel-spheres is shown in Fig. 2. The aging time was selected as 60 min. The density of Li_2CO_3 in gel-spheres increased with decreasing aging temperature between −20°C and room temperature. When the aging temperature was less than −20°C, the maximum density of Li_2CO_3 spheres was about 55% T.D. From evaluation of aging time and temperature, an aging condition of 60 min and less than −20°C was selected.

3.1.2. Calcination of gel-spheres

The calcination temperature was determined for removing PVA in the gel-spheres. The gel-spheres were heated in air at each temperature (100, 200, 300, 400, 500 and 600°C) for 6 h as the 3rd experiment. After heating, the gel-spheres were weighed and the grain size of the gel-spheres was observed by SEM. The relationship between calcination temperature and residual content of PVA in the gel-spheres and the relationship between calcination temperature and the grain size of Li_2CO_3 particles is shown in Fig. 3. At temperatures up to 300°C, PVA in the gel-spheres was not removed and the surface of the spheres was light brown. At 400, 500 and 600°C, greater than 95 wt% of the PVA was removed from the gel-spheres and the surface of

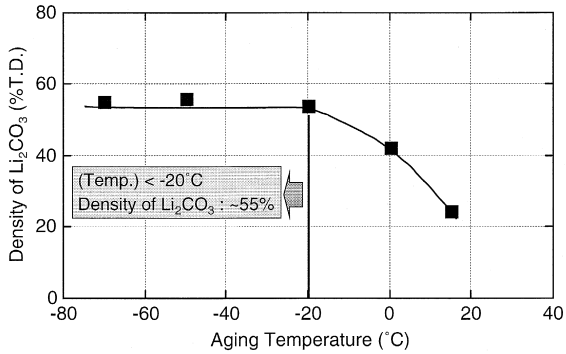

Fig. 2. Density dependence on the aging temperature of Li_2CO_3 in gel-spheres.

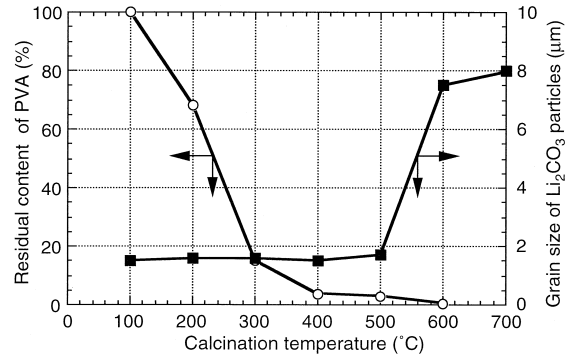

Fig. 3. Relationship between calcination temperature and residual content of PVA in gel-spheres and the relationship between calcination temperature and grain size of Li_2CO_3 particles.

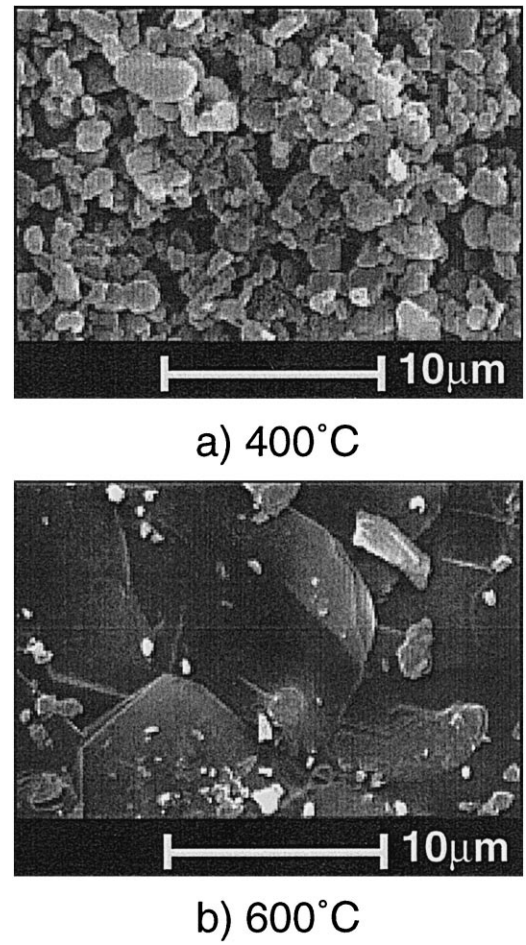

Fig. 4. SEM photographs of Li_2CO_3 spheres after calcination showing grain growth.

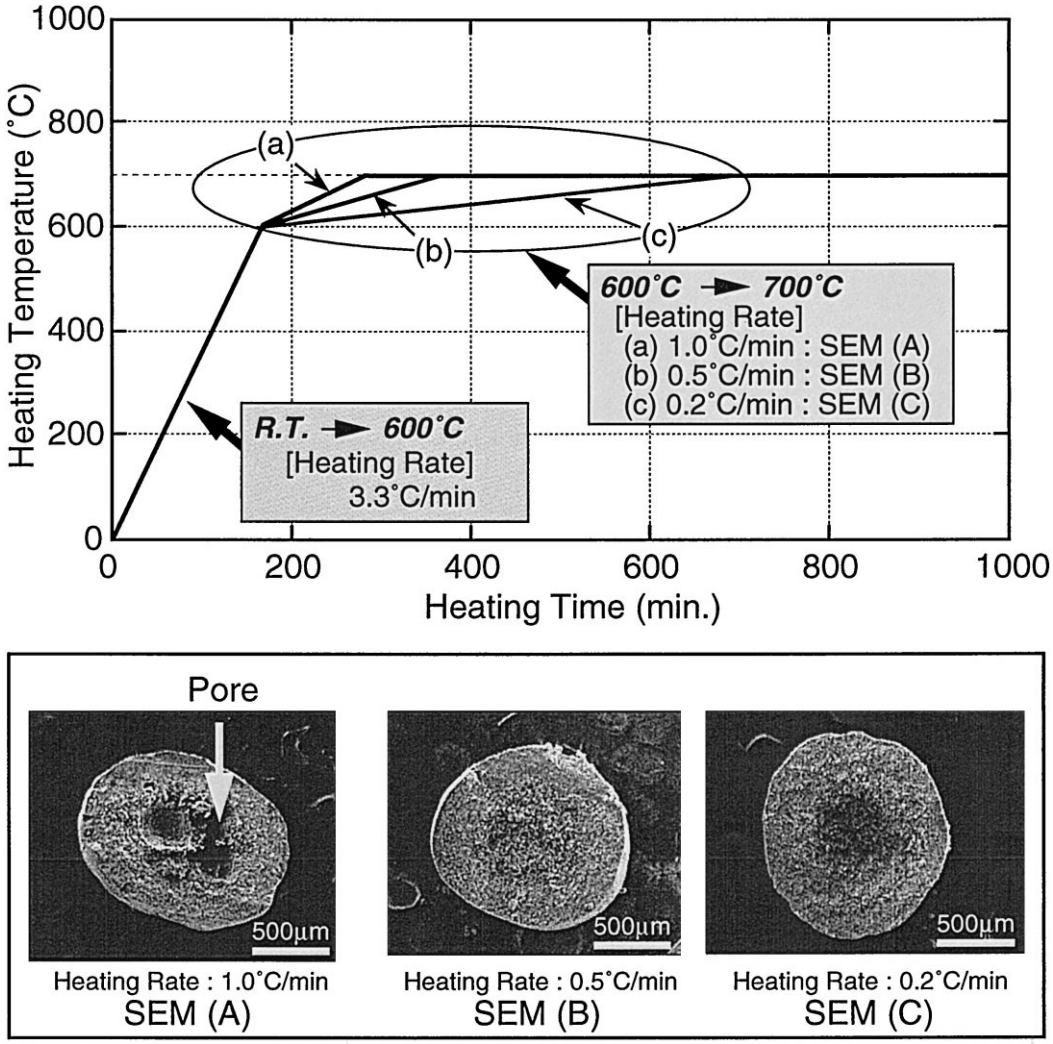

Fig. 5. Heating rate conditions during calcination and SEM photographs of Li_2O pebbles after thermal decomposition.

the spheres was white. Diffraction peaks corresponding to Li_2CO_3 were observed after heating at temperatures above 400°C. After calcination the material is referred to as 'Li_2CO_3 spheres' instead of 'gel-spheres'. SEM photographs of Li_2CO_3 spheres after calcination are shown in Fig. 4. At 400°C in Fig. 4, the grain size of Li_2CO_3 particles was about 1 μm. At the 600°C, the grain size of the Li_2CO_3 particles was about 8 μm. If grain growth affects the density of Li_2O pebbles, then an optimum calcination temperature can be selected.

3.1.3. Thermal decomposition and sintering

The Li_2CO_3 spheres were heated in vacuum and transformed to Li_2O. The thermal decomposition of Li_2CO_3 is

Table 2
Relationship between sintering temperature and weight loss of Li_2O pebbles

Sintering temperature (°C)	Density (% T.D.)	Weight of Li_2O pebbles (g)		Weight loss of Li_2O (%)
		before sintering	after sintering	
1100	80	3.6779	3.1243	15
1150	86	3.4391	2.0644	40
1200	–	5.3555	0.1383	97

Table 3
Characterization of Li_2O pebbles

Properties	Measuring methods	Measuring values
Density	liquid immersion method (Hg)	80% T.D.
Sphericity	photographic analysis	1.15 (av.) (see Fig. 6)
Crystal structure	XD analysis	XD pattern (see Fig. 8)
Pebble diameter	sieve classification	1.06 mm (av.)
Impurity content	ICP analysis	content (see Table 4)
Collapse load	autograph	1.74 kgf (av.) (see Fig. 7)

described in Ref. [14] and the transformation reaction can be written as

$$Li_2CO_3(s) \rightarrow Li_2O(s) + CO_2(g). \quad (1)$$

The Li_2CO_3 spheres were evacuated and heated until the temperature increased to 700°C at a heating speed of 3.3°C/min. After this process, the crystal structure of the spheres was determined by XRD and Li_2O was the main component detected. After thermal decomposition, weight loss of the spheres was 41.0 ± 0.4 wt%. The theoretical value obtained from Eq. (1) is 41.1 wt%.

Sintering tests were performed for 4 h at 1100°C with the Li_2CO_3 spheres fabricated at two calcination temperatures of 400 and 600°C. When the Li_2CO_3 spheres fabricated at 600°C were used, the size of the spheres decreased between the fabrication of the gel-spheres and calcination. From SEM photographs of Li_2O pebbles, when the Li_2CO_3 spheres were calcinated at 600°C, pores were observed in the inner part of Li_2O pebbles and the density of Li_2O pebbles was 65% T.D. On the other hand, the pores decreased in Li_2CO_3 spheres calcined at 400°C. The size of the spheres decreased after the thermal decomposition and the density of the Li_2O pebbles was improved up to 71% T.D. Carbon content in the Li_2O pebbles was measured by infrared absorptiometric method and was about 2 ppm. From these tests, grain growth in the Li_2CO_3 spheres decreases the density of Li_2O pebbles and, therefore, a calcination temperature of 400°C was chosen.

The calcination heating rate was evaluated in the 4th experiment. The pebble condition as a function of the heating rate during thermal decomposition and SEM photographs of Li_2O pebbles after thermal decomposition is shown in Fig. 5. Pores were observed in the inner part of Li_2O pebbles when the temperature increased to 600°C at 3.3°C/min and porosity increased from 600 to 700°C at 1.0°C/min. However, pores decreased in the inner part of Li_2O pebbles when the temperature increased from 600 to 700°C at a heating rate of less than 0.5°C/min. It appears that the internal homogeneous structure of Li_2O pebbles can be attributed to performing the thermal decomposition reaction at the slower rate.

Sintering was conducted in vacuum at a temperature range of 1100 to 1200°C for 4 h for the 5th experiment. The relationship between the sintering temperature and weight loss of Li_2O pebbles is shown in Table 2. As the sintering temperature increased, the density of Li_2O pebbles also increased. At a sintering temperature of 1200°C for 4 h, Li_2O was almost completely evaporated. The density and weight loss of Li_2O pebbles were 80% T.D. and 15 wt% at 1100°C for 4 h, respectively. On the other hand, the density and weight loss of Li_2O pebbles were 86% T.D. and 40 wt% at 1150°C for 4 h, respectively.

3.2. Characterization of Li_2O pebbles

A characterization of Li_2O pebbles fabricated in the fourth experiment was carried out. A summary on the characterization of Li_2O pebbles is shown in Table 3. The main features are discussed below.

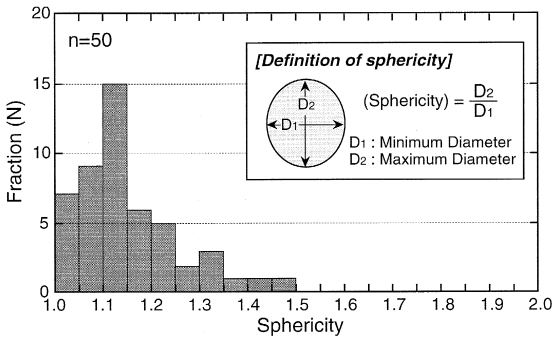

Fig. 6. Distribution of sphericity of Li_2O pebbles fabricated in the 4th experiment.

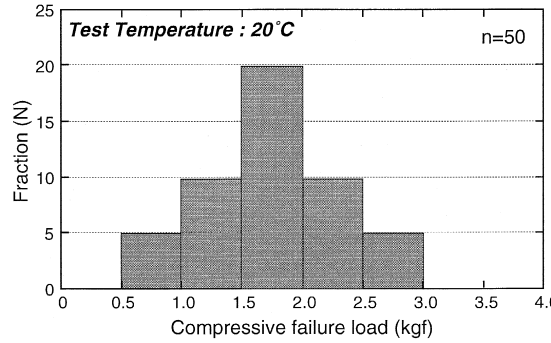

Fig. 7. Distribution of compressive failure load of Li_2O pebbles fabricated in the 4th experiment.

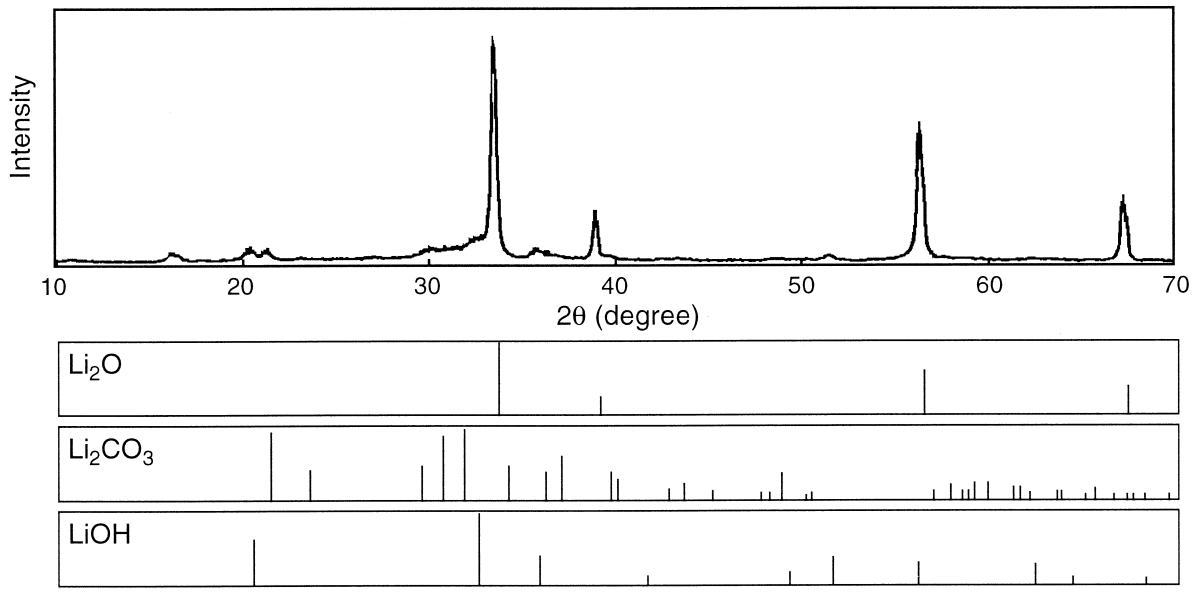

Fig. 8. X-ray diffraction pattern of Li_2O pebbles.

The density of Li_2O pebbles fabricated by this method was 80% T.D. The average size of Li_2O pebbles was 1.06 ± 0.05 mm. Sphericity of the Li_2O pebbles, which is the ratio of maximum to minimum diameter, was measured using a photographic analysis method. The distribution on the sphericity of Li_2O pebbles fabricated in the 4th experiment is shown in Fig. 6. The average sphericity of Li_2O pebbles was 1.15 ± 0.10 and the Li_2O pebbles are very spherical from Fig. 6. The distribution of a compressive failure load of Li_2O pebbles fabricated in the 4th experiment is shown in Fig. 7. The average compressive failure load was 1.74 ± 0.51 kgf. The X-ray diffraction pattern of Li_2O pebbles is shown in Fig. 8. From XRD analysis, Li_2O was the main component detected. The chemical composition of Li_2O pebbles is shown in Table 4 and aluminium and silicon were the highest impurities detected.

Table 4
Chemical composition of Li_2O pebbles

Elements	Contents (ppm)
Na	< 10
Mg	12
Ca	26
Fe	16
Cr	2
Ni	< 5
Al	60
Si	120
Pt	< 10
Cu	2
Bo	< 0.5
B	< 5
U	< 0.1

From the results of these tests, potential methods for fabricating small Li_2O pebbles with reasonable density were obtained.

4. Conclusion

Process improvement tests for making small Li_2O pebbles were carried out by a wet process in this study. The main conclusions are as follows.

(1) The density of Li_2O pebbles was a function of aging temperature, calcination temperature, heating rate during thermal decomposition and sintering temperature. Careful control of aging temperature, calcination temperature, heating rate and sintering temperature were required to increase the density of Li_2O pebbles.

(2) The heating rate during thermal decomposition increased the Li_2O pebble density. When the temperature increased to 600°C at 3.3°C/min and increased from 600 to 700°C at less than 0.5°C/min, pores decreased in the inner part of Li_2O pebbles and the Li_2O pebbles had a homogeneous structure. In this test, densities of Li_2O pebbles were obtained in the target range of 80 to 85% T.D.

(3) The characterization of Li_2O pebbles fabricated using the optimized parameters was carried out. The average size of Li_2O pebbles was 1.06 mm and the resulting sphericity was 1.15, with 1.0 being a perfect sphere.

From the results of these tests, Li_2O pebbles were fabricated with a density in the target range and bright

prospects exist concerning the fabrication process of small Li_2O pebbles by this wet method. In the future, fabrication processes of other ceramic breeders such as Li_2TiO_3 will be established and an automatic-control dropping system of gel-spheres will be designed and developed for a mass production process.

Acknowledgements

We greatly appreciate the helpful comments on this paper by Dr O. Baba (Director, Department of JMTR, JAERI).

References

[1] C.E. Johnson, K.R. Kummerer, E. Roth, J. Nucl. Mater. 155–157 (1988) 188.
[2] C.E. Johnson, G.W. Hollenberg, N. Roux, H. Watanabe, Fusion Eng. Des. 8 (1989) 145.
[3] T. Takahashi, H. Watanabe, Fusion Eng. Des. 8 (1989) 399.
[4] M.S. Ortman, E.M. Larsen, J. Am. Ceram. Soc. 66 (1983) 645.
[5] B.J.F. Palmer, J.D. Sullivan, C.W. Turner, J.D. Halliday, Adv. Ceram. 25 (1987) 149.
[6] T. Suzuki, O. Murata, S. Hirata, Ceram. Trans. 27 (1991) 37.
[7] N. Asami, K. Nagashima, H. Akiyama, M. Nagakura, N. Suemori, A. Ohya, Ceram. Trans. 27 (1991) 17.
[8] K. Tsuchiya, H. Kawamura, M. Nakamichi, H. Imaizumi, M. Saito, T. Kanzawa, M. Nagakura, J. Nucl. Mater. 219 (1995) 240.
[9] K. Tsuchiya, H. Kawamura, M. Saito, K. Tatenuma, M. Kainose, J. Nucl. Mater. 219 (1995) 246.
[10] C.W. Turner, B.C. Clatworthy, Adv. Ceram. 27 (1991) 149.
[11] O. Renoult, J.P. Boilot, J.P. Korb, D. Petit, M. Boncoeur, J. Nucl. Mater. 219 (1995) 233.
[12] O. Renoult, J.P. Boilot, J.P. Korb, M. Boncoeur, J. Nucl. Mater. 223 (1995) 126.
[13] K. Tsuchiya, H. Kawamura et al., SOFE '95, 16th IEEE/NPSS Symp. on Fusion Engineering, 1995, p. 1123.
[14] T. Takahashi, H. Watanabe, Fusion Eng. Des. 8 (1989) 399.